



OPEN ACCESS

EDITED BY

Francesca Di Sole,
Des Moines University, United States

REVIEWED BY

Victor Babich,
Mercy College of Health Sciences,
United States
Gilles Crambert,
ERL8228 Métabolisme et Physiologie
Rénales, France

*CORRESPONDENCE

Li-Ming Chen,
✉ liming.chen@hust.edu.cn
Ying Liu,
✉ liuying@hust.edu.cn

SPECIALTY SECTION

This article was submitted to Renal
Physiology and Pathophysiology,
a section of the journal
Frontiers in Physiology

RECEIVED 31 January 2023

ACCEPTED 24 March 2023

PUBLISHED 04 April 2023

CITATION

Cai L, Wang D, Gui T, Wang X, Zhao L,
Boron WF, Chen L-M and Liu Y (2023),
Dietary sodium enhances the expression
of SLC4 family transporters, IRBIT, L-
IRBIT, and PP1 in rat kidney: Insights into
the molecular mechanism for renal
sodium handling.
Front. Physiol. 14:1154694.
doi: 10.3389/fphys.2023.1154694

COPYRIGHT

© 2023 Cai, Wang, Gui, Wang, Zhao,
Boron, Chen and Liu. This is an open-
access article distributed under the terms
of the [Creative Commons Attribution
License \(CC BY\)](https://creativecommons.org/licenses/by/4.0/). The use, distribution or
reproduction in other forums is
permitted, provided the original author(s)
and the copyright owner(s) are credited
and that the original publication in this
journal is cited, in accordance with
accepted academic practice. No use,
distribution or reproduction is permitted
which does not comply with these terms.

Dietary sodium enhances the expression of SLC4 family transporters, IRBIT, L-IRBIT, and PP1 in rat kidney: Insights into the molecular mechanism for renal sodium handling

Lu Cai¹, Dengke Wang², Tianxiang Gui¹, Xiaoyu Wang¹,
Lingyu Zhao¹, Walter F. Boron², Li-Ming Chen^{1*} and Ying Liu^{1*}

¹Key Laboratory of Molecular Biophysics of Ministry of Education, School of Life Science and Technology, Huazhong University of Science and Technology, Wuhan, Hubei, China, ²Department of Physiology and Biophysics, Case Western Reserve University School of Medicine, Cleveland, OH, United States

The kidney plays a central role in maintaining the fluid and electrolyte homeostasis in the body. Bicarbonate transporters NBCn1, NBCn2, and AE2 are expressed at the basolateral membrane of the medullary thick ascending limb (mTAL). In a previous study, NBCn1, NBCn2, and AE2 are proposed to play as a regulatory pathway to decrease NaCl reabsorption in the mTAL under high salt condition. When heterologously expressed, the activity of these transporters could be stimulated by the InsP3R binding protein released with inositol 1,4,5-trisphosphate (IRBIT), L-IRBIT (collectively the IRBITs), or protein phosphatase PP1. In the present study, we characterized by immunofluorescence the expression and localization of the IRBITs, and PP1 in rat kidney. Our data showed that the IRBITs were predominantly expressed from the mTAL through the distal renal tubules. PP1 was predominantly expressed in the TAL, but is also present in high abundance from the distal convoluted tubule through the medullary collecting duct. Western blotting analyses showed that the abundances of NBCn1, NBCn2, and AE2 as well as the IRBITs and PP1 were greatly upregulated in rat kidney by dietary sodium. Co-immunoprecipitation study provided the evidence for protein interaction between NBCn1 and L-IRBIT in rat kidney. Taken together, our data suggest that the IRBITs and PP1 play an important role in sodium handling in the kidney. We propose that the IRBITs and PP1 stimulates NBCn1, NBCn2, and AE2 in the basolateral mTAL to inhibit sodium reabsorption under high sodium condition. Our study provides important insights into understanding the molecular mechanism for the regulation of sodium homeostasis in the body.

KEYWORDS

solute carriers (SLC), Na⁺-bicarbonate cotransporter, SLC4A2, SLC4A7, SLC4A10, thick ascending limb of Henle's loop, Na⁺-Cl⁻ cotransporter NCC, renal sodium reabsorption

Introduction

The kidney maintains the systemic homeostasis of fluid and electrolytes in the body, and therefore plays a central role in the long-term control of arterial blood pressure (Guyton, 1989; Gonzalez-Vicente et al., 2019). The systemic sodium content is a key factor that determines the volume of blood and extracellular fluid. Sodium retention would increase the blood volume, which in turn would increase the arterial blood pressure. Most of, if not all, the monogenic forms of hypertension are associated with aberrant renal function in sodium handling (Wadei and Textor, 2012).

The thick ascending limb (TAL) reabsorbs ~25%–30% of the NaCl filtered by the glomerulus (Dimke and Schnermann, 2018; Gonzalez-Vicente et al., 2019). The entry of vast majority of the Na⁺ and Cl⁻ into the epithelial cells is accounted for by the apical furosemide-sensitive Na⁺-K⁺-Cl⁻ cotransporter NKCC2 (SLC12A1) and the Na⁺-H⁺ exchanger NHE3 (SLC9A3) in the TAL. In the basolateral membrane, Na⁺ is extruded by the Na⁺-K⁺-ATPase, whereas Cl⁻ enters the interstitial fluid *via* the chloride channel CLC-K (for review, see refs. (Bazua-Valenti et al., 2016; Gonzalez-Vicente et al., 2019). Loss-of-function mutations in NKCC2 causes hypotension due to urinary waste of salt, whereas overactivity of NKCC2 results in hypertension (Ji et al., 2008; Ares et al., 2011). In the TAL, NKCC2 is stimulated upon phosphorylation by the SPS/Ste20-related proline-alanine-rich kinase (SPAK), which is phosphorylated by the with-no-Lys kinase WNK (Mutig, 2017; Caceres and Ortiz, 2019). Loss-of-function mutations in WNK and SPAK are associated with hypotension (Richardson and Alessi, 2008; Murthy et al., 2017; Shekarabi et al., 2017).

Genetics studies show that a number of bicarbonate transporters of the solute carrier 4 (SLC4) family are associated with hypertension. These include *SLC4A1* encoding the Cl⁻-HCO₃⁻ exchanger AE1 (Kokubo et al., 2006), *SLC4A2* encoding AE2 (Sober et al., 2009), *SLC4A4* encoding the Na⁺-HCO₃⁻ cotransporter NBCe1 (Yang et al., 2012; Guo et al., 2016), *SLC4A5* encoding NBCe2 (Barkley et al., 2004; Carey et al., 2012; Groger et al., 2012), and *SLC4A7* encoding NBCn1 (Ehret et al., 2011; Lu et al., 2015). *SLC4A10* encoding NBCn2 is associated with the regulation of systemic fluid balance (Boger et al., 2017).

The abovementioned SLC4 family members are all expressed in the kidney, making a major contribution to the regulation of systemic acid-base balance in the body. In rat kidney, the activities of Cl⁻-HCO₃⁻ exchange and Na⁺-dependent HCO₃⁻ transport are both expressed in the basolateral membrane of the medullary (m) TAL (Kikeri et al., 1990; Bourgeois et al., 2002; Odgaard et al., 2004). In the basolateral mTAL, the Cl⁻-HCO₃⁻ exchange activity is attributable to the expression of AE2 (Alper et al., 1997), whereas the Na-HCO₃⁻ cotransport activity is attributable to NBCn1 and NBCn2 (Kim et al., 2003; Praetorius et al., 2004; Guo et al., 2017). AE2 mediates the extrusion of HCO₃⁻ during the transepithelial HCO₃⁻ reabsorption in the mTAL (Bourgeois et al., 2002). In rat kidney, the abundances of NBCn1, NBCn2, and AE2 are upregulated by overload of NaCl or NaHCO₃ (Quentin et al., 2004; Wang J. L. et al., 2020). NaHCO₃ overload induces metabolic alkalosis. As an adaptive response to metabolic alkalosis, the HCO₃⁻ reabsorption in the mTAL would be expected to be downregulated. The upregulation in AE2 by NaHCO₃ appears

to contradict the role of AE2 in HCO₃⁻ reabsorption. Similar to NaCl, administration of NaHCO₃ also causes sodium overload. Thus, it is proposed that, under high sodium condition, the NBCs (NBCn1 and NBCn2) together with AE2 inhibit NaCl reabsorption by counteracting the action of the apical NKCC2 and the basolateral Na⁺-K⁺ ATPase in mTAL (Wang J. L. et al., 2020).

When heterologously expressed in *Xenopus* oocytes, the activities of NBCn1 and NBCn2 are greatly stimulated by protein interaction with the InsP3R binding protein released with inositol 1,4,5-trisphosphate (IRBIT) and L-IRBIT (Wang J. L. et al., 2020). Both IRBIT and L-IRBIT could interact with AE2. The expression and activity of AE2 is stimulated by L-IRBIT, but not IRBIT in human embryonic kidney HEK-293 cells (Itoh et al., 2021). In rat kidney, the expression of IRBIT and L-IRBIT is upregulated under high salt condition (Wang J. L. et al., 2020). In HEK-293 cells, the activity of NBCn1 is downregulated by SPAK and upregulated by protein phosphatase 1 (PP1) (Hong et al., 2013).

Taken together, the above studies suggest the presence of a potential regulatory network involved in the modulation of NaCl reabsorption in the mTAL. However, some major gaps in knowledge remain to be addressed. Are IRBIT, L-IRBIT, and PP1 expressed in the mTAL where NBCn1, NBCn2, and AE2 are localized? Is there an effect of chloride in the upregulation of renal NBCn1, NBCn2, and AE2 by NaCl overload? Would the expression of the bicarbonate transporters and their regulatory partners be affected by varying just the dietary sodium content? In the present study, we investigated the localization of NBCn1, IRBIT, L-IRBIT, and PP1 in rat kidney by immunofluorescence. We also examined the effect of altering dietary sodium on the protein expression of selected transporters and their potential regulators in rat kidney. Our data indicate that the abundances of these proteins in the kidney are closely correlated with the dietary sodium intake.

Methods

Animals and ethical approval

Sprague Dawley (SD) rats were purchased from the Hubei Provincial Center for Disease Control (Wuhan, China) and housed in rodent cages. *Xenopus laevis* clawed frogs were purchased from Shanghai Institute of Biochemistry and Cell Biology, Chinese Academy of Sciences (Shanghai, China) and housed in a fish tank at 18°C. All procedures regarding the usage of experimental animals were approved by the Institutional Committee on Animal Care and Use at Huazhong University of Science and Technology.

Rodent chows were purchased from Trophic Animal Feed High-tech Co. Ltd. (Nantong, Jiangsu, China). The standard chow (AIN93M) contained 0.1% Na⁺. The high-sodium chow contained 1%, 2%, or 3% Na⁺. All chows with varying sodium levels were carefully balanced to keep the chloride unchanged in the chow.

To examine the effect of dietary sodium on the kidney, adult SD rats weighing 200–300 g were randomly assigned into 4 groups. Each group contained at least 8 rats. The control group received standard AIN93 chow containing 0.1% of Na⁺. The other groups

received modified chow containing 1%, 2%, or 3% sodium, respectively. All rats had free access to drinking water. After 10 days of treatment, the rats were anesthetized by subcutaneous injection of pentobarbital sodium (2% w/v) and sacrificed for tissue collection. The tissues were immediately frozen in liquid nitrogen upon isolation and stored at -80°C until usage.

Antibodies

The polyclonal antibody anti-NBCn2 was described previously (Guo et al., 2017). This anti-NBCn2 was directed against the unique Nt of MEIK-NBCn2 (Liu et al., 2013) that is expressed at the basolateral membrane of mTAL (Guo et al., 2017). The polyclonal antibodies anti-NBCn1 and anti-L-IRBIT were described in a previous study (Wang J. L. et al., 2020). Polyclonal rabbit anti-IRBIT was commercially available (catalogue no. 94248S; Cell Signaling Technology, Danvers, MA, USA). Mouse anti-actin was purchased from Beyotime (catalogue no. AA128; Haimen, China). Rabbit anti-AE2 was purchased from ABclonal (catalogue no. A7729; Wuhan, China). Rabbit anti-PP1C β (catalogue no. ab53315), mouse anti- α 1 (catalogue no. AB7671), and mouse anti-calbindin (catalogue no. ab82812) were purchased from Abcam (Shanghai, China). Rabbit anti-pNCC for phosphorylated NCC was purchased from PhosphoSolutions (catalogue no. p1311-53; Aurora, CO, USA). Mouse anti-NKCC2 was purchased from Santa Cruz (catalogue no. sc-293222; Santa Cruz, California, USA).

HRP-conjugated goat anti-rabbit IgG (catalogue no. A0218) and goat anti-mouse IgG (catalogue no. A0216) were purchased from Beyotime (Haining, Jiangsu, China). DyLight549-conjugated goat anti-rabbit IgG catalogue no. A23320 and DyLight488-conjugated goat anti-mouse IgG (catalogue no. A23210) were purchased from Abbkine Scientific (Wuhan, China).

Protein preparation and Western blotting

For protein preparation, a rat kidney tissue of about 500 mg was placed in 6 mL of precooled protein isolation buffer (in mM: 7.5 NaH_2PO_4 , 250 sucrose, 5 EDTA, 5 EGTA, pH 7.0) supplemented with 1% protease inhibitor cocktail (catalog no. P8340; Sigma-Aldrich, St. Louis, MO, USA). The tissue was homogenized for 15 strokes with a Glas-Col Teflon glass homogenizer (Glas-Col, Terre Haute, IN, USA) bathed in ice. The crude homogenate was centrifuged at 3,000g for 10 min at 4°C to remove the cell debris. A vial of the resultant supernatant was saved, representing the “total proteins.” The membrane proteins were pelleted from the supernatant by ultra-centrifuged at $100,000\times g$ for 60 min at 4°C and resuspended in a buffer containing 20 mM Tris, 5 mM EDTA, 5% SDS, pH 8.0. Protein concentration was determined by using Enhanced BCA Protein Assay Kit (catalog no. P0010; Beyotime). The protein preparations were stored in aliquots at -80°C until usage.

Proteins were separated by sodium dodecyl sulfate polyacrylamide gel electrophoresis (SDS-PAGE) and blotted onto a PVDF membrane for Western blotting. The blot was blocked with 5% milk in $1\times$ TBST (1 mM Tris, 150 mM NaCl, 0.1% Tween 20, pH 7.4) for 1 h at room temperature (RT), incubated with primary

antibody in $1\times$ TBST containing 1% milk, and then washed five times with $1\times$ TBST. The blot was then incubated with HRP-conjugated secondary antibody in $1\times$ TBST containing 1% milk at RT and washed five times with $1\times$ TBST. Chemiluminescence was performed with SuperSignal West Pico PLUS Chemiluminescent Substrate (catalogue no. 3580, Thermo Scientific, Rockford, IL, USA) prior to X-ray film exposure. Densitometry was performed with ImageJ (National Institutes of Health, USA).

Tissue fixation and immunofluorescence

Adult rats were fixed by transcardial perfusion with 4% paraformaldehyde (PFA) in PBS (in mM: 77.4 Na_2HPO_4 , 22.6 NaH_2PO_4 , pH 7.4). For immunofluorescence, cryo-sections of kidney were cut with thickness of 8 μm . The section was dehydrated overnight at 60°C and then rehydrated for 1 h in $1\times$ TBS (1 mM Tris, 150 mM NaCl, pH 7.4). After five 5-min washes with $1\times$ TBS, the section was incubated in Improved Citrate Antigen Retrieval Solution (catalogue no. P0083; Beyotime) at 98°C for 20 min. After five 5-min washes with $1\times$ TBS, the section was then blocked for 1 h with Immunol Staining Blocking Buffer (catalogue no. P0102; Beyotime) at RT, and incubated with primary antibody at 4°C overnight. The section was washed five times with $1\times$ TBS, incubated with DyLight-conjugated secondary antibody at room temperature for 1 h followed by five washes with $1\times$ TBS, and then mounted with Antifade Polyvinyl Pyrrolidone Medium (catalogue no. P0131; Beyotime). The mounting medium contains 4,6-Diamidino-2-Phenylindole (DAPI). Images were acquired on a FluoView FV3000 confocal microscope (Olympus, Tokyo, Japan).

Molecular biology

Construction of vectors was performed by regular molecular cloning approaches. For generation of the constructs for yeast-2-hybrid, the cDNA encoding mouse IRBIT (accession no. NM_145542) was fused in-frame to the DNA-binding domain of the transcription factor GAL4 in pGBKT7. The cDNA encoding the amino-terminal portion (residues 1–115) of NBCn1 (accession no. AKS30237.1) was fused in-frame to the activation domain of GAL4 in pGADT7.

For generation of the constructs for expression in *Xenopus* oocytes, the target cDNA was subcloned into pGH19 which contained the T7 promoter for transcription (Trudeau et al., 1995). The plasmid containing the cDNA encoding NBCe1-B tagged with EGFP at the carboxyl-terminus was described previously (Su et al., 2021). All constructs used for electrophysiology analysis were tagged with EGFP at the carboxyl-termini. The constructs were linearized for the preparation of capped cRNAs by *in vitro* transcription with T7 mMessage mMachine kit (Ambion, Austin, TX, USA).

Yeast two-hybrid

Yeast two-hybrid (Y2H) was performed with Matchmaker[®] Gold Yeast Two-Hybrid System (catalog no. PT4084-1, Clontech

Takara, Mountain View, CA, USA) to investigate the protein interaction between IRBIT and NBCn1. Vectors pGBKT7 (expressing IRBIT) and pGADT7 (expressing NBCn1 Nt) were transformed into haploid yeast strains Y2HGold and Y187, respectively. Y187 and Y2HGold were mated to form diploid and then cultured on either double-dropout (DDO) medium lacking or quadruple-dropout (QDO) medium containing X- α -gal at 30°C for 3–4 days. Protein interaction was judged by the formation of blue colonies.

Electrophysiology recordings

Xenopus oocytes were used as expression system for electrophysiology recordings. For oocyte isolation, a female *Xenopus laevis* was anesthetized by immersion in 0.2% ethyl 3-aminobenzoate methanesulfonate or tricaine (catalog no. A5040, Sigma-Aldrich, St. Louis, MO, USA). An ovary lobe was isolated and digested with 2 mg/mL collagenase Type 1A (Sigma-Aldrich, St. Louis, MO, USA) in Ca²⁺-free NRS solution (in mM: 82 NaCl, 2 KCl, 20 MgCl₂, 5 HEPES, pH 7.50) for 90 min at room temperature. Stage V–VI oocytes were selected for usage. cRNA injection into oocytes was performed with Nanoject II Auto-Nanoliter Injector (Drummond Scientific Company, Broomall, PA, USA). For protein expression, the oocytes injected with cRNA were incubated at 18°C for 4–5 days in modified Gibco™ Leibovitz's L-15 Medium (catalog no. 41300-039, Thermo Fisher Scientific, Waltham, MA, USA) containing 100 units/mL of Gibco™ penicillin and 100 μ g/mL of streptomycin (Thermo Fisher Scientific,) with 200 mOsm osmolarity.

Two-electrode voltage clamp were performed with an OC-725C oocyte clamp (Warner Instruments, Hamden, CT, USA) controlled by pCLAMP10.2 (Molecular Devices, San Jose, CA, USA). For voltage-clamp recordings, an oocyte was placed in nominally “HCO₃⁻-free” ND96 (in mM: 96 NaCl, 2 KCl, 1 MgCl₂, 1.8 CaCl₂, 5 HEPES, pH 7.5, 200 mOsm) in a chamber and impaled with two microelectrodes filled with 3 M KCl, one for sensing membrane potential (*V_m*) and the other for measuring current. The cell was equilibrated in ND96 until the *V_m* reached stable. The activity of NBCe1 was determined as previously described (Su et al., 2021). Briefly, the current-voltage (I-V) relationships were first acquired for ND96 solution and then for a CO₂/HCO₃⁻ solution (in mM: 63 NaCl, 2 KCl, 1 MgCl₂, 1.8 CaCl₂, 5 HEPES, 33 NaHCO₃ bubbled with 5% CO₂, pH 7.50). The difference between the current in ND96 and that in CO₂/HCO₃⁻ represented the net HCO₃⁻-dependent current mediated by NBCe1. The slope conductance (*G_{NBC}*) of this net I-V curve between \pm 40 mV was an index for NBCe1 activity.

Co-immunoprecipitation

For co-immunoprecipitation, 2.5 mg of membrane proteins of rat kidney were mixture with 1 μ L of antibody against L-IRBIT in 1.2 mL of IP buffer (in mM: 20 Tris, 150 NaCl, 2 EDTA, pH 7.5) containing 1% (v/v) Triton X-100 and 1% (v/v) protease inhibitor cocktail (Sigma-Aldrich) and incubated at 4°C overnight. The

mixture was then added with Dynabeads™ M-280 Sheep anti-Rabbit IgG (catalog no. 11204D, Thermo Fisher Scientific) and incubated for 2 h at room temperature. After 3 \times washes with the IP buffer, the beads were resuspended in 60 μ L of SDS sample buffer and incubated at 98°C for 10 min. The supernatant was collected for Western blotting analysis.

Data analysis

Statistical analyses were performed with GraphPad Prism (GraphPad Software, Inc. URL: www.graphpad.com).

Results

NBCn1 is expressed in mTAL, but not in cTAL of rat kidney

It has been established that NBCn1 is expressed in the basolateral membrane of mTAL (Praetorius et al., 2004; Wang J. L. et al., 2020). What remains uncertain is whether NBCn1 is expressed in tubular segments beyond the mTAL. In a previous study, we showed by Western blotting that NBCn1 expression is largely limited to the outer medulla in rat kidney (Wang J. L. et al., 2020). A comprehensive RNA-seq study showed that, in addition to mTAL, *Slc4a7* transcripts are also expressed in the descending (DTL), ascending thin limb (ATL) of the Henle's loop, and cTAL in mouse kidney (Chen et al., 2021; URL: esbl.nhlbi.nih.gov/MRECA/Nephron/). In the present study, we examined the tissue and cellular distribution of NBCn1 in rat kidney by immunofluorescence. We used NKCC2 as a specific marker for the TAL (Ecelbarger et al., 1996; Gimenez and Forbush, 2003; Bazua-Valenti et al., 2016). Figures 1A–C show the overview of double staining of anti-NBCn1 and anti-NKCC2 in a kidney section. The fluorescence signals for NBCn1 were highly enriched in the outer medulla, but not present in the cortex or the inner medulla. High magnification view showed that the expression of NBCn1 was highly abundant in most of the mTAL (Figure 1D) but became much lower in the TAL segments approaching the cortex (Figure 1E), indicating expression heterogeneity in the mTAL. Figure 1F shows the absence of NBCn1 staining in the cTAL. The present immunofluorescence data are consistent with our previous Western blotting data (Wang J. L. et al., 2020), but are somewhat inconsistent with the RNA-seq data obtained from mouse kidney (Chen et al., 2021). The inconsistency could be due to the application of different technical approaches. It could also reflect the species specificity in the expression of *SLC4A7* in the kidney.

Expression and localization of IRBIT in rat kidney

The α 1 subunit of the Na⁺-K⁺-ATPase is expressed in virtually all segments along the nephron, with the highest abundance from the mTAL through the cortical connecting tubule (CNT) (Wetzel and Sweadner, 2001; Bankir et al., 2020). We utilized α 1 as a marker to determine the localization of IRBIT in rat kidney. Figure 2A shows the

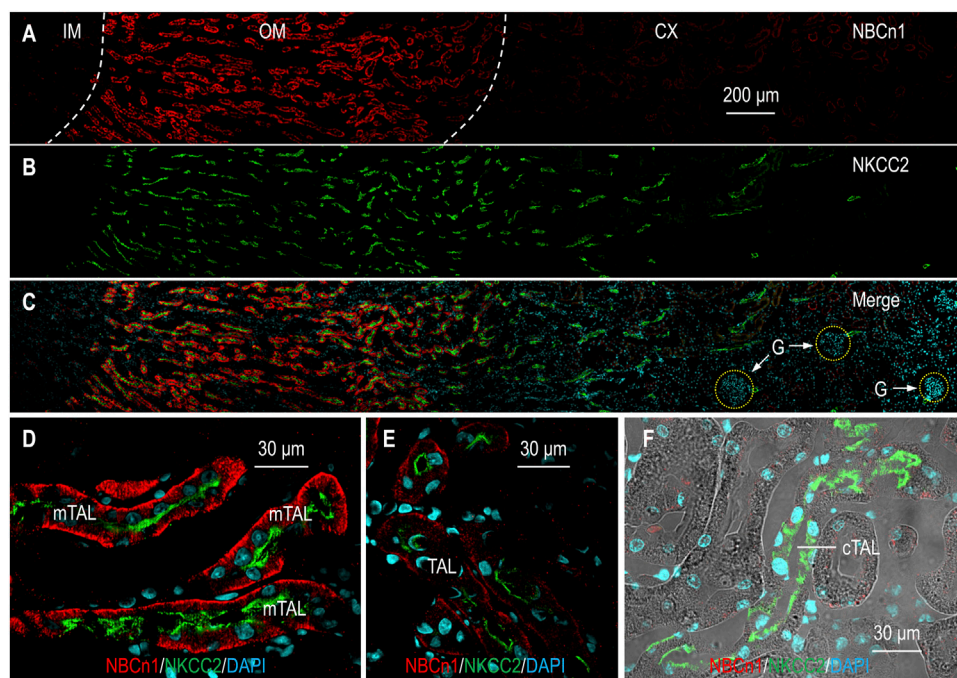


FIGURE 1

Indirect immunofluorescence of NBCn1 in rat kidney. (A–C) Overview of the double staining of NBCn1 and NKCC2 in a rat kidney section. To provide a whole view of the tissue distribution of NBCn1 (red) and NKCC2 (green), the figure was generated by overlaying four continuous images acquired from the inner medulla through the cortex. NKCC2 was present along the whole TAL from the OM through the CX. The fluorescence signal of NBCn1 was strong in the OM, relatively weak in the OM–CX boundary region, and negligible in the CX. (D) NBCn1 was highly expressed in the basolateral domain of mTAL. (E) NBCn1 was expressed in relatively lower level in the basolateral domain of the TAL in the OM–CX boundary region. (F) NBCn1 was not detectable in the cortical TAL. IM, inner medulla; OM, outer medulla; CX, cortex; G, glomerulus. The blue indicates nuclei counter-stained by DAPI.

overview of the double staining of anti-IRBIT and anti- $\alpha 1$ in a kidney section (also see [Supplementary Figure S1](#)). IRBIT was predominantly expressed in the outer medulla and the inner portion of the cortex. The fluorescence signals of IRBIT were also present in specific structures in the outer portion of the cortex, but very weak in the inner medulla.

High magnification view showed that the expression of IRBIT was highly enriched in the mTAL that was intensively labeled by $\alpha 1$ ([Figures 2B–D](#)). A double-staining with IRBIT and NKCC2 confirmed the expression of IRBIT in the mTAL ([Figures 2E–G](#)).

[Figures 2H–J](#) shows the double-staining of IRBIT and $\alpha 1$ in the cortex. Here, strong immunofluorescence signals of IRBIT were observed in the tubules intensively labeled by anti- $\alpha 1$, indicating IRBIT expression in the cTAL through the cortical collecting duct (CCD). The expression of IRBIT in the cTAL was confirmed by double-staining with anti-IRBIT and anti-NKCC2 (data not shown). In the cortex, IRBIT was also abundantly expressed in the proximal tubules. The abundance of IRBIT appeared higher in the PST and the CCD than it was in the proximal convoluted tubules (PCT). Note that, the abundance of $\alpha 1$ was highest in the CCD, lower in the PCT, and even lower in the PST. The fluorescence signal of IRBIT was very faint in the glomeruli.

We further characterized the localization of IRBIT in the cortex by co-staining with calbindin. The Ca^{2+} -binding-protein calbindin is a specific marker for the distal convoluted tubules (DCT) through the CCD, with highest abundance in the CNT, and lower in the DCT and CCD ([Campean et al., 2001](#); [Wetzel and Sweadner, 2001](#)). [Supplementary Figures S2A–C](#) illustrates the representative

staining of IRBIT and calbindin in renal cortex. IRBIT was highly enriched in the tubules positive with calbindin. In [Supplementary Figures S2D–F](#), the tubules with the highest expression of calbindin were presumably the CNT, whereas the structures with relatively lower level of calbindin were presumably the CCD. Taken together, the calbindin data show that IRBIT was abundantly expressed in the DCT through the CNT in the renal cortex.

[Supplementary Figures S3A–D](#) shows the double-staining of IRBIT and NKCC2 in the cortex of the kidney. Here, IRBIT was expressed in the NKCC2-positive cTAL reaching the macula densa, a specialized tubule juxtaglomerular that plays a critical role for sensing the NaCl content in the tubular fluid ([Peti-Peterdi and Harris, 2010](#)). The tubules with IRBIT expression but lacking NKCC2 were presumably the CNT. [Supplementary Figures S3E–H](#) shows the double-staining for IRBIT and calbindin around a glomerulus. Here, the juxtaglomerular structure strongly labeled by IRBIT but lacking calbindin was presumably the cTAL, whereas those with both IRBIT and calbindin were presumably the CNTs.

Expression and localization of L-IRBIT in rat kidney

[Figure 3A](#) shows the overview of the double-staining of L-IRBIT and $\alpha 1$ in a kidney section (also see [Supplementary Figure S4](#)). Our

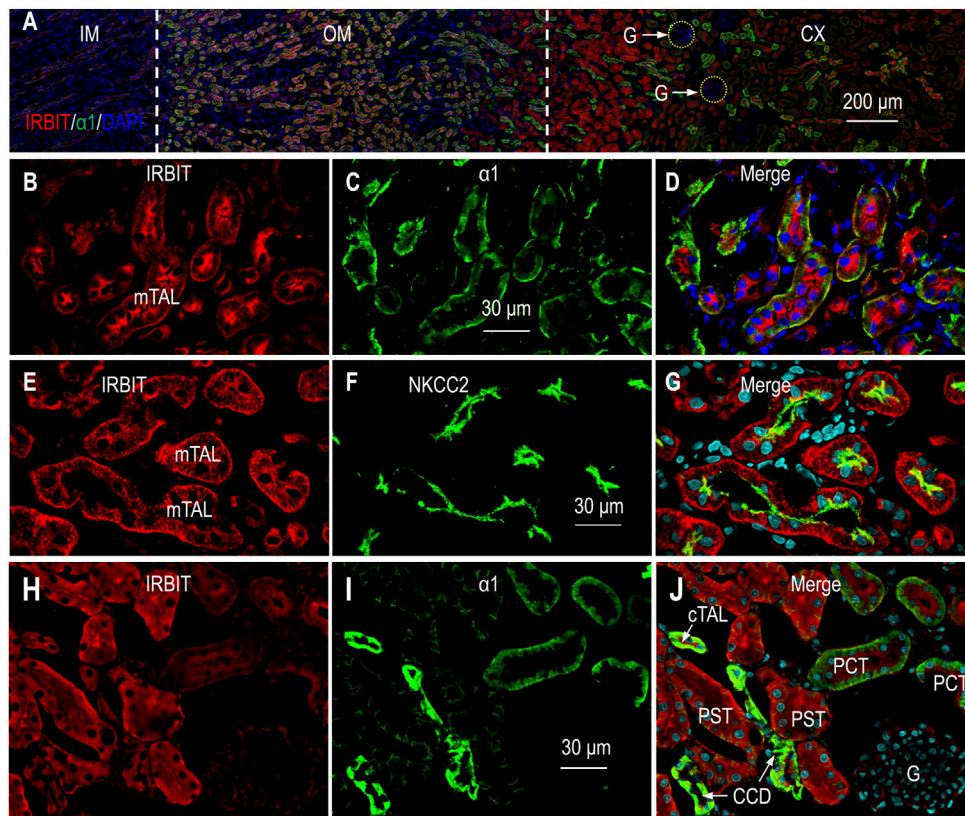


FIGURE 2

Indirect immunofluorescence of IRBIT in rat kidney. (A) Merged overview of double staining of IRBIT (red) and $\alpha 1$ (green) in a rat kidney section. The original unmerged images of IRBIT and $\alpha 1$ were shown in [Supplementary Figure S1](#). (B–D) High magnification view showing that IRBIT is abundantly expressed in mTAL. (E–G) Localization of IRBIT and NKCC2 in mTAL. (H–J) Localization of IRBIT (red) and $\alpha 1$ (green) in cortex. G, glomerulus; mTAL, medullary thick ascending limb; CX, cortex; OM, outer medulla; IM, inner medulla. Blue indicates the nuclei counter-stained with DAPI.

data show that L-IRBIT was widely expressed from the outer medulla throughout the cortex. Similar to the case of IRBIT, the immunofluorescence signals of L-IRBIT were weak in the inner medulla.

[Figures 3B–D](#) represent the high magnification view of L-IRBIT staining in the outer medulla. Here, L-IRBIT was highly enriched in the mTAL intensively labeled by $\alpha 1$. L-IRBIT expression was also observed in relatively lower abundance in the outer medullary collecting duct (OMCD) that was only slightly labeled by $\alpha 1$. [Figures 3E–G](#) show the double-staining of L-IRBIT and NKCC2 in the outer medulla. Here, strong signals of L-IRBIT were observed in the mTAL with NKCC2 at the apical domain, as well as in the OMCD lacking NKCC2.

In the cortex, L-IRBIT was ubiquitously expressed in high abundance in the PST with the lowest level of $\alpha 1$, the PCT modestly labeled by $\alpha 1$, and the cTAL and the CCD with the highest level of $\alpha 1$ ([Figures 3H–J](#)). [Supplementary Figures S5A–C](#) shows the double-staining for L-IRBIT and calbindin in the cortex. The abundance of L-IRBIT was slightly higher in the tubules with calbindin than those without calbindin. [Supplementary Figures S5D–F](#) shows the expression of L-IRBIT in NKCC2-positive cTAL.

Taking together, we conclude that L-IRBIT was predominantly expressed from the TAL through the CCD, and was also expressed in relatively lower level in the PCT and the PST in rat kidney.

Expression and localization of PP1 in rat kidney

[Figure 4A](#) shows the overview of the double staining of anti-PP1 and anti- $\alpha 1$ in a kidney section (also see [Supplementary Figure S6](#)). The inner medulla was slightly labeled by anti-PP1. In the outer medulla and the cortex, the immunofluorescence signals of PP1 were most intensive in the tubules with the highest levels of $\alpha 1$, suggesting that PP1 expression was enriched from the mTAL through the CCD. [Figures 4B–D](#) shows PP1 staining in the outer medulla in high magnification view. Here, PP1 was most abundantly expressed in the mTAL with high levels of $\alpha 1$. PP1 was also expressed in high abundance in the OMCD, the basolateral domain of which was slightly labeled by anti- $\alpha 1$.

In the cortex, strong signals of PP1 were observed in the tubules intensively labeled by $\alpha 1$, suggesting that PP1 was highly expressed from the cTAL through the CCD ([Figures 4E–G](#)). In the cortex, PP1 signals were always seen in the tubules positive with calbindin, confirming the expression of PP1 in the DCT, CNT, and CCD ([Supplementary Figures S7A–C](#)). Taking together, we conclude that PP1 was predominantly expressed from cTAL through CCD in renal cortex.

Finally, the expression of PP1 was also present in the glomeruli ([Figures 4E–G](#); [Supplementary Figure S7](#)).

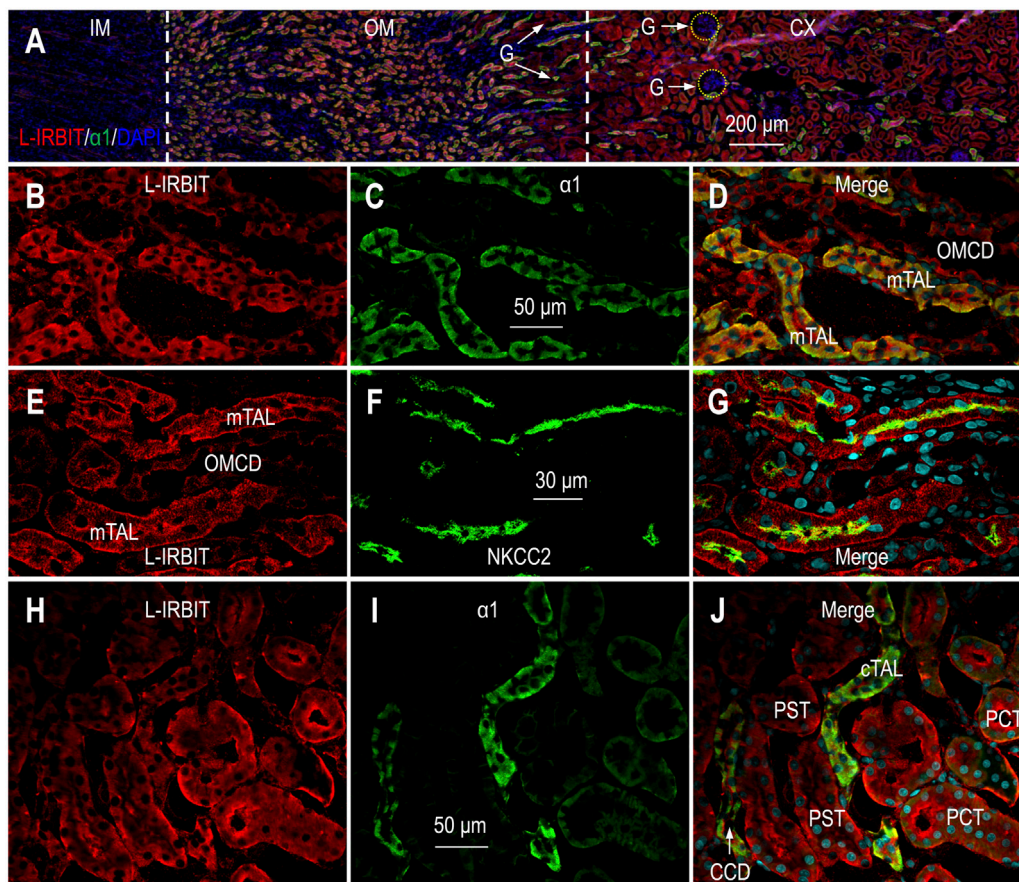


FIGURE 3

Indirect immunofluorescence of L-IRBIT in rat kidney. (A) Merged overview of the double-staining of L-IRBIT (red) and $\alpha 1$ (green). The original unmerged images of L-IRBIT and $\alpha 1$ were shown in [Supplementary Figure S4](#). (B–D) Localization of L-IRBIT and $\alpha 1$ of $\text{Na}^+ - \text{K}^+ - \text{ATPase}$ in outer medulla. (E–G) Localization of L-IRBIT and NKCC2 in outer medulla. (H–J) Localization of L-IRBIT (red) and $\alpha 1$ (green) in cortex. CX, cortex; IM, inner medulla; OM, outer medulla; mTAL, medullary thick ascending limb; OMCD, outer medullary collecting duct. Blue indicates the nuclei counter-stained by DAPI.

Effect of dietary sodium on expression of transporters in rat kidney

We examined the effect of dietary sodium on the expression of selected transporters in rat kidney. Adult rats were treated for 10 days either with standard rodent chow containing 0.1% Na^+ or modified rodent chow containing high sodium. The membrane preparations of whole kidneys were used for Western blotting analyses.

[Figure 5A](#) shows representative Western blots for the expression of renal NBCn1. As summarized in [Figure 5B](#), compared to the control (1.00 ± 0.27), the relative abundances of NBCn1 in the high-sodium groups were significantly increased to 1.78 ± 0.38 for 1% Na^+ , 2.20 ± 1.24 for 2% Na^+ , and 3.05 ± 0.89 for 3% Na^+ , respectively. By regression analysis, the relative abundance of NBCn1 was significantly positively correlated with the level of dietary sodium ($r^2 = 0.485$, $p < 0.0001$).

Shown in [Figure 5C](#) are representative Western blots for the expression of NBCn2 in the kidney. As summarized in [Figure 5D](#), compared to the control (1.00 ± 0.74), the relative abundances of NBCn2 were significantly increased to 2.18 ± 0.86 for 1% Na^+ , 3.09 ± 1.13 for 2% Na^+ , and 3.74 ± 2.63 for 3% Na^+ , respectively. Again, by

regression analysis, the relative abundance of NBCn2 was significantly positively correlated with the level of dietary sodium ($r^2 = 0.330$, $p = 0.006$).

[Figure 5E](#) shows representative Western blots for the effect of dietary sodium on the expression of renal AE2. Compared to the control, the abundances of AE2 were so strikingly increased that the AE2 in the control was almost invisible even when the AE2 was over-exposed in the high-sodium groups. Thus, it was not practical to obtain the relative ratio of AE2 of the high-sodium groups over the control.

Finally, we examined the effect of dietary sodium on the expression of Na-Cl cotransporter NCC (SLC12A3) in rat kidney. NCC is the major transporter in the capical DCT responsible for NaCl reabsorption by the DCT ([Murthy et al., 2017](#); [Shekarabi et al., 2017](#)). Phosphorylation increases the activity of NCC ([Glover et al., 2010](#)). Others have shown that high-salt diet decreases the abundance of phosphorylated NCC (pNCC) in mouse kidney ([Torres-Pinzon et al., 2021](#)). Shown in [Figure 5F](#) are representative Western blots for the expression of pNCC in rat kidney. As summarized in [Figure 5G](#), compared to the control (1.00 ± 0.66), the relative abundances of pNCC in the high-sodium groups were decreased to 0.66 ± 0.37 for 1% Na^+ , 0.40 ± 0.28 for 2% Na^+ , and 0.24 ± 0.16 for 3% Na^+ , respectively. The decreases for the

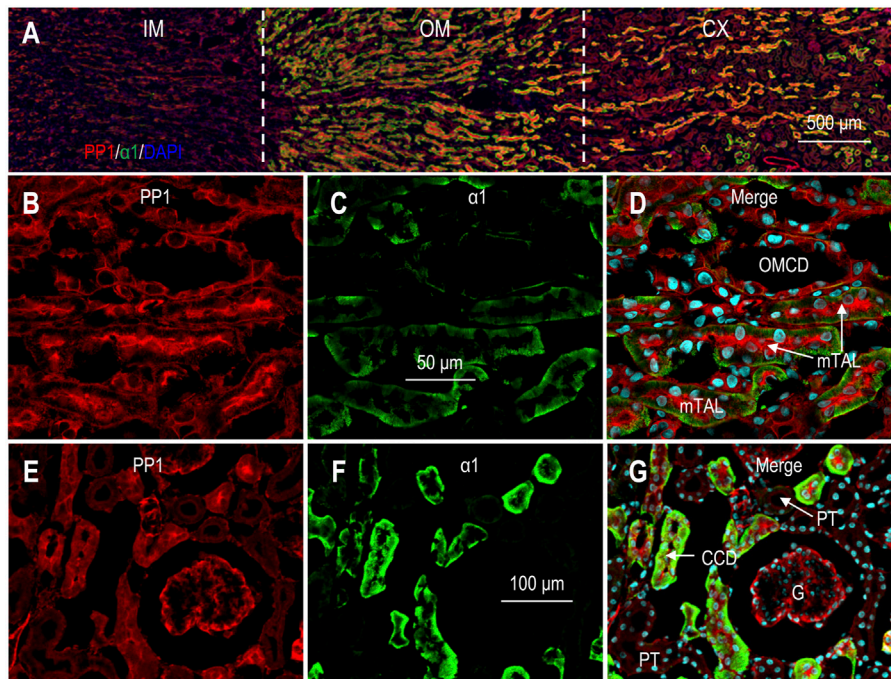


FIGURE 4

Indirect immunofluorescence of PP1 in rat kidney. **(A)** Merged overview of the double-staining of PP1 and $\alpha 1$ in rat kidney. The original unmerged images of PP1 and $\alpha 1$ were shown in [Supplementary Figure S6](#). **(B–D)** Expression of PP1 and $\alpha 1$ in out medulla. Strong fluorescence signals of PP1 were observed in the mTAL and the OMCD. **(E–G)** Expression of PP1 and $\alpha 1$ in cortex. Fluorescence signals of PP1 were observed in the glomerulus and the cortical collecting duct. G, glomerulus; CCD, cortical collecting duct; mTAL, medullary thick ascending limb; OMCD, outer medullary collecting duct.

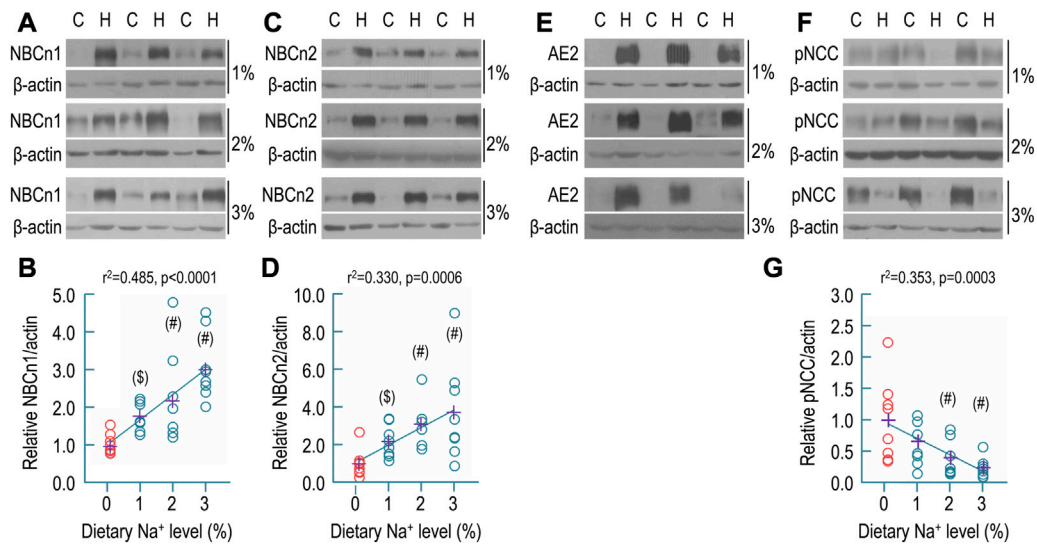


FIGURE 5

Effect of dietary sodium on the expression of NBCn1, NBCn2, AE2, and pNCC in rat kidney. **(A)** Representative western blots for the expression of NBCn1 in the kidney. **(B)** Summary for the relative abundance of renal NBCn1. **(C)** Representative western blots for the expression of NBCn2 in the kidney. **(D)** Summary for the relative abundance of renal NBCn2. **(E)** Representative western blots for the expression of AE2 in the kidney. The abundance of AE2 was strikingly increased by dietary sodium. It was not practical to determine the relative ratio of AE2 abundance of high sodium groups over the control. **(F)** Representative western blots for the expression of pNCC in the kidney. **(G)** Summary for the relative abundance of renal pNCC. Western blotting analyses were performed with the membrane preparations of whole kidney. C: control normal (0.1% Na⁺). H: high sodium diet. Each data point (circles) represents an individual rat ($n = 8$ for each condition). The data points of the control (0.1% of Na⁺) are presented in red. The crosses in purple indicate the means of protein levels in each condition. #: significantly different from the control (red) by one-way ANOVA followed by Dunnett's multiple comparison ($p < 0.05$). \$: significantly different from the control by Student's *t*-test ($p < 0.05$).

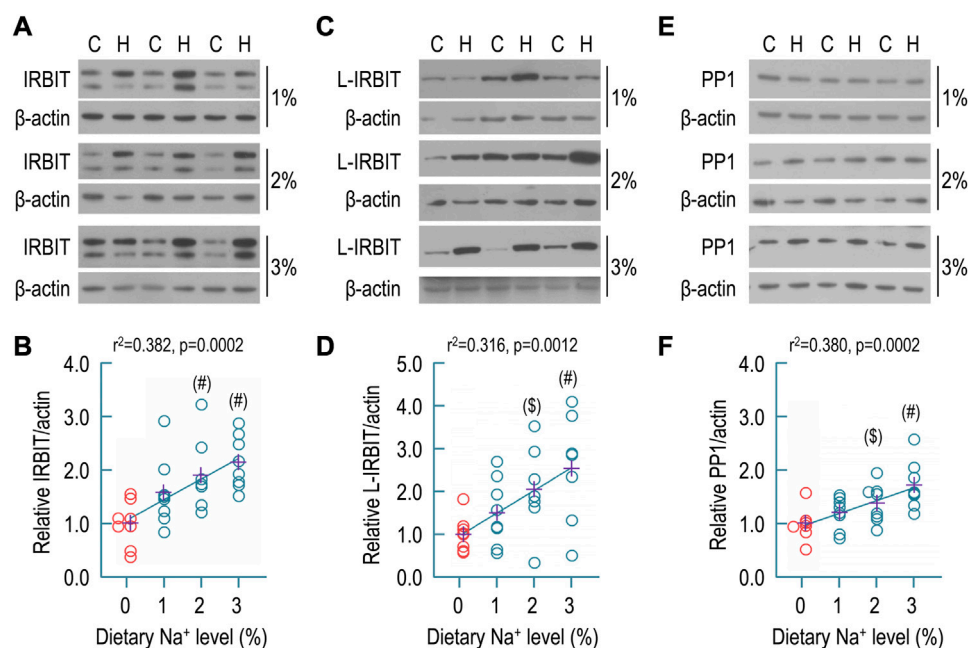


FIGURE 6

Effect of dietary sodium on expression of IRBIT, L-IRBIT, and PP1 in rat kidney. **(A)** Representative Western blots for the expression of IRBIT in the kidney. **(B)** Summary for the relative abundance of renal IRBIT. **(C)** Representative Western blots for the expression of L-IRBIT in the kidney. **(D)** Summary for the relative abundance of renal L-IRBIT. **(E)** Representative western blots for the expression of PP1 in the kidney. **(F)** Summary for the relative abundance of renal PP1. Western blotting analyses were performed with the membrane preparations of whole kidney. C: control normal (0.1% Na⁺); H: high sodium diet. Each data point represents an individual rat ($n = 7-8$ for each condition). The data points of the control (0.1% of Na⁺) are presented in red. The crosses in purple indicate the means of protein levels in each condition. #: significantly different from the control (red) of 0.1% Na⁺ by one-way ANOVA followed by Dunnett's multiple comparison ($p < 0.05$). \$: significantly different from the control by Student's *t*-test ($p < 0.05$). In Panel **(B)** (the condition of 0.1% Na⁺), and Panel **(F)** (the conditions of 0.1% and 2% Na⁺), several data points were artificially shifted to left because these were virtually overlapped with other data points.

groups of 2% and 3% Na⁺ are statistically significant compared to the control. Moreover, the relative abundance of pNCC in rat kidney was significantly negatively correlated with dietary sodium level by regression analysis ($r^2 = 0.353$, $p = 0.0003$). Our data are consistent with the previous study on mice (Torres-Pinzon et al., 2021).

Effect of dietary sodium on expression of IRBIT, L-IRBIT, and PP1 in rat kidney

Next, we examined the effect of dietary sodium on the expression of IRBIT, L-IRBIT, and PP1 in the membrane preparations of whole rat kidney. Shown in Figure 6A are representative Western blots for the expression of IRBIT in the kidney. As summarized in Figure 6B, compared to the control (1.00 ± 0.42), the relative abundances of IRBIT were increased to 1.58 ± 0.65 for 1% Na⁺, 1.90 ± 0.65 for 2% Na⁺, and 2.15 ± 0.49 for 3% Na⁺, respectively. The increases in the groups of 2% and 3% Na⁺ are statistically compared to the control. Moreover, the relative abundance of renal IRBIT was significantly positively correlated to the level of dietary sodium by regression analysis ($r^2 = 0.382$, $p = 0.0002$).

Similar analyses were performed with L-IRBIT. Shown in Figure 6C are representative Western blots for the expression of L-IRBIT in rat kidney. As summarized in Figure 6D, compared to

the control (1.00 ± 0.41), the relative abundances of L-IRBIT were increased to 1.51 ± 0.78 for 1% Na⁺, 2.05 ± 1.03 for 2% Na⁺, and 2.54 ± 1.28 for 3% Na⁺, respectively. The increases in the groups of 2% and 3% Na⁺ were statistically significant compared to the control. Moreover, the relative abundance of L-IRBIT was significantly positively correlated to the level of dietary sodium by regression analysis ($r^2 = 0.316$, $p = 0.0012$).

Figure 6E shows representative Western blots for PP1 expression in rat kidney. As summarized in Figure 6F, compared to the control (1.00 ± 0.29), the relative abundances of PP1 were increased to 1.20 ± 0.30 for 1% Na⁺, 1.38 ± 0.36 for 2% Na⁺, and 1.72 ± 0.44 for 3% Na⁺, respectively. The increases in the groups of 2% and 3% Na⁺ are statistically significant compared to the control. Again, the relative abundance of renal PP1 was significantly positively correlated to dietary sodium level by regression analysis ($r^2 = 0.380$, $p = 0.0002$).

Interaction of NBCn1 with IRBIT/L-IRBIT

IRBIT and L-IRBIT (collectively the IRBITs) can bind to and greatly stimulate the activities of many NBCs, such as NBCe1-B, NBCn1, and NBCn2. These NBCs all contain an auto-inhibition domain (AID) as well as an IRBIT-binding domain at the flexible amino-termini (for review, see refs. (Parker and Boron, 2013; Liu

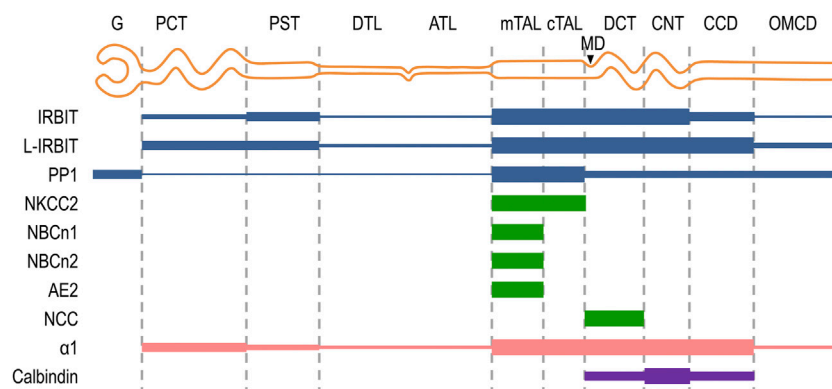


FIGURE 8

Schematic diagram summarizing the localization of NBCn1, IRBIT, L-IRBIT, PP1, NKCC2 along the nephron. The expression localizations of IRBIT, L-IRBIT, and PP1 in the kidney were systematically characterized for the first time in the present study. The expression of NBCn1, NBCn2 and AE2 in the mTAL was established previously (Alper et al., 1997; Kim et al., 2003; Praetorius et al., 2004; Guo et al., 2017). The present study confirmed the localization of NBCn1 in the mTAL, but not in other segments of the nephron. The specific localization of NCC in DCT was established previously (Campean et al., 2001). NKCC2 is a specific marker for the mTAL and cTAL (Ecelbarger et al., 1996; Gimenez and Forbush, 2003). Calbindin is a specific marker for DCT, CNT, and CCD (Campean et al., 2001; Wetzel and Sweadner, 2001). G, glomerulus; PCT, proximal convoluted tubule; PST, proximal straight tubule; DTL, descending thin limb; ATL, ascending thin limb; mTAL, medullary thick ascending limb; cTAL, cortical thick ascending limb; MD, macula densa; DCT, distal convoluted tubule; CNT, cortical connecting tubule; CCD, cortical collecting duct; OMCD, outer medullary collecting duct.

these constructs \pm IRBIT by electrophysiology. Generally, the electrophysiology data confirmed the conclusion derived from the Y2H data (Figure 7D). For example, based on AID_{n1}- Δ N85, replacing “DEEAVVD” with “AAAAAAA” (construct #5) abolished the stimulation of the transporter by IRBIT ($1.93 \pm 0.80 \mu\text{S}$ without IRBIT vs. $1.61 \pm 0.37 \mu\text{S}$ with IRBIT, $p > 0.05$), suggesting that “DEEAVVD” is essential for the interaction of NBCn1 with IRBIT. Again, replacing the basic cluster of NBCn1 with that of NBCe1-B (construct #3) abolished the stimulation of the transporter by IRBIT ($9.34 \pm 2.87 \mu\text{S}$ without IRBIT vs. $9.75 \pm 3.25 \mu\text{S}$ with IRBIT, $p > 0.05$). However, in the absence of IRBIT, the basal activity of construct #3 is significantly higher than that of wild-type NBCe1-B, suggesting lower magnitude of auto-inhibition for construct #3.

Taken together, the above Y2H and electrophysiology data suggest that the interaction of NBCn1 with IRBIT requires the acidic motif “DEEAVVD” and the basic cluster in NBCn1. Moreover, it is essential to maintain sufficient number of alkaline residues in the basic cluster for the effective interaction between NBCn1 and IRBIT.

Finally, by co-immunoprecipitation with anti-L-IRBIT, we obtained NBCn1 from rat kidney (Figure 7E). It is proposed that the IRBITs are involved in the regulation of NBCn1 and NBCn2 in the kidney (Wang J. L. et al., 2020). The co-immunoprecipitation data suggest the presence of protein interaction between NBCn1 and L-IRBIT in rat kidney.

Discussion

In the present study, we performed a careful characterization for the expression and localization of NBCn1, IRBIT, L-IRBIT, and PP1 in rat kidney. As summarized in Figure 8, the expression of NBCn1 is limited to the mTAL along the nephron. IRBIT and

L-IRBIT are expressed almost everywhere along the nephron in rat kidney. The expression of IRBIT is most abundant from the mTAL through the CNT, relatively lower in the PST and the CCD, and even lower in other regions of the nephron. The expression of L-IRBIT is most abundant from the mTAL through the CCD, relatively lower in the PCT and the PST, and even lower in other regions of the nephron. PP1 is most abundant in the TAL, and relatively lower from the DCT through the MCD. PP1 is also expressed in high abundance in the glomerulus.

The expression of NBCn1, NBCn2, and AE2 are significantly stimulated by increasing dietary sodium intake, whereas the abundance of pNCC is significantly decreased by dietary sodium. Finally, the abundance of IRBIT, L-IRBIT, and PP1 are positively correlated to dietary sodium intake.

The role of NBCn1, NBCn2, and AE2 in renal sodium handling

The SLC4 family transporters NBCn1, NBCn2, and AE2 are all expressed in the basolateral membrane of mTAL (Alper et al., 1997; Kim et al., 2003; Praetorius et al., 2004; Guo et al., 2017). In a previous study (Wang J. L. et al., 2020), the authors have proposed that NBCn1, NBCn2, and AE2 are involved in the regulation of NaCl handling by mTAL. According to the model in this previous study, the NBCs (NBCn1 and NBCn2) by coordination with AE2 mediate the back flux of Na⁺ and Cl⁻ under high salt condition, counteracting the NaCl reabsorption mediated by the apical NKCC2, the basolateral Na⁺-K⁺-ATPase and Cl⁻ channel. Supporting this theory are the following lines of observations. Firstly, NaCl overload upregulates the expression of NBCn1, NBCn2, and AE2 in rat kidney (Quentin et al., 2004; Wang J. L. et al., 2020). Secondly, NaHCO₃ overload upregulates the expression of AE2 in rat kidney (Quentin et al., 2004). Finally, NaHCO₃ upregulates the expression of renal NBCn1 and NBCn2 with a greater effect than NaCl does (Wang J. L. et al., 2020). The stimulatory effect of NaHCO₃

on AE2 expression disagrees with its role in HCO_3^- reabsorption inasmuch as an upregulation in AE2 would increase the capacity of HCO_3^- reabsorption of the mTAL, causing further alkalosis. However, the upregulation of AE2 by NaHCO_3 could be well explained by the proposed role of AE2 in NaCl reabsorption.

In the previous study (Wang J. L. et al., 2020), the greater effect of NaHCO_3 on the expression of NBCn1 and NBCn2 than NaCl indicates a net effect of sodium. In the present study, we find the abundances of renal NBCn1 and NBCn2 are proportionally upregulated by increasing dietary sodium intake. The abundance of renal AE2 is also strikingly upregulated by increasing dietary sodium. These new findings further corroborate the idea that NBCn1 and NBCn2 together with AE2 inhibit renal reabsorption of NaCl under high salt condition. Moreover, the new findings indicate that sodium is the major factor that accounts for the upregulation of these bicarbonate transporters under high salt condition.

Dysfunctions of *SLC4A2* encoding AE2 and *SLC4A7* encoding NBCn1 are associated with hypertension (Sober et al., 2009; Boedtker et al., 2011; Ehret et al., 2011; Wang et al., 2017). The inhibitory role of NBCn1 and AE2 in renal sodium reabsorption indicates that the development of hypertension associated with the dysfunction of *SLC4A7* and *SLC4A2* could be the result of renal sodium retention. Nevertheless, the development of hypertension is often a multifactorial event. Others have shown that NBCn1 is involved in the regulation of the contraction of blood vessel smooth muscle (Boedtker et al., 2011; Jiang et al., 2019), indicating the presence of a cardiovascular component in the development of hypertension caused by the dysfunction of *SLC4A7*.

The role of IRBIT in renal sodium handling

IRBIT is able to interact with and regulate the function of a series of proteins with distinct physiological functions. The binding partners of IRBIT include membrane channels, such as the endoplasmic reticulum Ca^{2+} channel (InsP3R) and cystic fibrosis transmembrane conductance regulator (CFTR), and membrane transporters such as NHE3 (He et al., 2008; He et al., 2010; Tran et al., 2013; He et al., 2016), NBCe1-B (Shirakabe et al., 2006), NBCn1 (Hong et al., 2013; Wang J. L. et al., 2020), NBCn2 (Wang J. L. et al., 2020), AE2 (Itoh et al., 2021), SLC26A6 (Park et al., 2013; Khamaysi et al., 2019), SLC13A2, Na^+ -succinate cotransporter SLC13A3 (Khamaysi et al., 2019), etc. IRBIT can also interact with protein kinases, such as calcium calmodulin-dependent kinase II alpha (CaMKII α) (Kawaai et al., 2015), as well as lipid kinases, such as PIPK1 α and PIPKII α (Ando et al., 2015).

Virtually all the above-mentioned channels and transporters that interact with IRBIT are expressed in the kidney. For example, NHE3 (SLC9A3) is expressed in the apical membrane of the proximal tubules and TAL, playing a major role in the regulation of acid-base balance and the reabsorption of Na^+ . NHE3 activity is stimulated by angiotensin II (Ang II) in a manner dependent on IRBIT and CaMKII α (He et al., 2010). NHE3 in the proximal tubule is shown to be involved in the development of hypertension induced by Ang II (Nwia et al., 2022). The apical SLC26A6 in the proximal tubule plays a dispensible role in the regulation of NaCl homeostasis in the body (Knauf et al., 2001; Knauf et al., 2019). The Na^+ /dicarboxylate cotransporter SLC13A2 is expressed in the apical

membrane of the proximal tubule in human kidney (Lee et al., 2017). Here, SLC13A2 forms complex with SLC26A6 (Ohana et al., 2013). The Na^+ -succinate cotransporter SLC13A3/NaDC-3 is abundantly expressed at the basolateral membrane of renal proximal tubule (Burckhardt et al., 2005; Breljak et al., 2016). In the distal segments of the nephron, CFTR in concert with SLC26A4 is involved in the regulation of HCO_3^- secretion under metabolic alkalosis (Berg et al., 2021a; Berg et al., 2021b).

In the present study, we find that IRBIT is almost ubiquitously expressed along the nephron. The wide distribution of IRBIT and its interaction partners in the kidney implies profound significance of IRBIT in renal physiology. It is conceivable that, in the kidney, IRBIT is involved in the regulation of many different physiological processes by regulating diverse target proteins. In the previous study (Wang J. L. et al., 2020), the authors have shown that NaCl overload generally upregulates the expression of IRBIT in rat kidney. In the present study, we show that the abundance of IRBIT is proportionally increased with the level of dietary sodium, indicating that sodium is the major factor that modulate the expression of renal IRBIT under high salt condition. We propose that IRBIT plays an important role to inhibit renal sodium reabsorption.

Given the demonstrated stimulatory effect of IRBIT on NBCn1, NBCn2 (Hong et al., 2013; Wang J. L. et al., 2020), it is possible that, under high sodium condition, IRBIT stimulates the activities of the basolateral NBCn1 and NBCn2—the expressions of which are upregulated under high sodium condition—to inhibit NaCl reabsorption in the mTAL.

IRBIT activates NBCe1-B by abolishing the action of the auto-inhibition domain at the amino-terminal end of NBCe1-B (Lee et al., 2012; Lee and Boron, 2018; Su et al., 2021). The auto-inhibition domains of NBCn1 and NBCn2 are homologous to that of NBCe1-B. It is very likely that IRBIT activates NBCn1 and NBCn2 by a molecular mechanism similar to that for NBCe1-B.

The role of L-IRBIT in renal sodium handling

L-IRBIT is highly homologous to IRBIT with more than 93% of sequence identity regardless of their unique Nt appendages. Given the high degree of sequence identity, it is very likely that L-IRBIT can interact with most of the binding partners of IRBIT (Kawaai et al., 2017). Previous studies have shown that L-IRBIT interacts with and stimulates the activities of NHE3 (Kawaai et al., 2017), NBCe1-B (Yamaguchi and Ishikawa, 2014; Wang M. et al., 2020), NBCn1 (Wang J. L. et al., 2020), NBCn2 (Wang J. L. et al., 2020), and AE2 (Itoh et al., 2021). L-IRBIT can also interact with CaMKII α and InsP3R (Kawaai et al., 2017).

In the present study, we find that L-IRBIT is almost ubiquitously expressed in the kidney. The broad distribution of L-IRBIT implies that L-IRBIT play diverse roles in renal physiology. Considering the fact that the abundance of L-IRBIT is proportionally upregulated by increasing dietary sodium, we propose that L-IRBIT plays an inhibitory role in renal sodium reabsorption under high sodium condition. Given the demonstrated stimulatory effect of L-IRBIT on NBCn1, NBCn2, and AE2 (Hong et al., 2013; Wang J. L. et al., 2020; Itoh et al., 2021), L-IRBIT could do so by stimulating the basolateral NBCn1, NBCn2, and AE2—the expressions of which are all upregulated under high sodium condition—in the mTAL, therefore increasing the back flux of Na^+ and Cl^- , thus decreasing the reabsorption of Na^+ and Cl^- .

The role of PP1 in renal sodium handling

In the present study, we show that PP1 is widely expressed along the nephron with the highest abundance in the TAL. The abundance of renal PP1 is proportionally downregulated by dietary sodium. We propose that PP1 plays an important role to inhibit renal sodium reabsorption under high sodium condition. Consistent with this hypothesis, knocking out the inhibitor-1 of PP1 causes hypotension in mouse (Picard et al., 2014).

PP1 could inhibit renal sodium reabsorption via diverse mechanisms depending on the specific segments of the nephron. When heterologously expressed in HeLa cells, the activity of NBCn1 is stimulated by PP1 and inhibited by kinase SPAK (Hong et al., 2013). The observations suggest that NBCn1 is activated by dephosphorylation. Given the expressional upregulation of both PP1 and NBCn1 by dietary sodium, we hypothesize that PP1 stimulates NBCn1 in mTAL, therefore inhibiting sodium reabsorption by the mTAL under high sodium condition. So far, little is known about the phosphorylation of NBCn1. The proposed activation of NBCn1 by PP1 call for future studies to address the molecular mechanism underlying the phosphorylation regulation of NBCn1.

Elsewhere, PP1 could inhibit renal sodium reabsorption by down-regulating the activity of the apical NCC in the DCT, where NCC plays a major role in NaCl reabsorption (for review, see refs. (Murthy et al., 2017; Shekarabi et al., 2017; Azlan et al., 2021). Others have shown that dephosphorylation decreases NCC activity in *Xenopus* oocytes (Glover et al., 2010) and in DCT epithelial cells (Picard et al., 2014). A number of studies have shown that PP1 is involved in the phosphorylation regulation of NCC in the kidney (Picard et al., 2014; Penton et al., 2019; Poulsen et al., 2021). Indeed, inhibition of PP1 by expressing I-1, a specific PP1 inhibitor, substantially increases the phosphorylation level as well as the activity of NCC in *Xenopus* oocytes (Picard et al., 2014). Consistently, knocking-out I-1 substantially decreases the phosphorylation level of NCC in mouse kidney (Picard et al., 2014; Penton et al., 2019). In the present study, we show that the renal abundance of pNCC (phosphorylated NCC) is decreased under high sodium intake, an observation consistent with previous studies (Shao et al., 2021; Torres-Pinzon et al., 2021). This decrease in pNCC is likely attributable to the increased expression of PP1.

Concluding remarks

The present study provided insights into the molecular network underlying the regulation of renal sodium handling. In the mTAL, NaCl reabsorption is facilitated by NKCC2 and NHE3 at the apical membrane, and inhibited by the SLC4 bicarbonate transporters NBCn1, NBCn2, and AE2 at the basolateral membrane. Under high sodium conditions, the bicarbonate transporters NBCn1, NBCn2, and AE2, at least some of them, could be functionally upregulated by protein interaction with the IRBITs and by dephosphorylation by, e.g., protein phosphatase PP1. The functional interaction between the bicarbonate transporters (e.g., NBCn1) and PP1 in the kidney remains to be addressed in future. Moreover, the molecular mechanism underlying the regulation of these bicarbonate transporters by phosphorylation/dephosphorylation remains unknown and calls for future studies. Finally, given the almost ubiquitous expression in the kidney, the IRBITs and PP1 could be

involved in the regulation of sodium handling in renal segments beyond the mTAL.

Data availability statement

The original contributions presented in the study are included in the article/Supplementary Materials, further inquiries can be directed to the corresponding authors.

Ethics statement

The animal study was reviewed and approved by Institutional Committee on Animal Care and Use at Huazhong University of Science and Technology.

Author contributions

YL and L-MC designed the study. LC performed the immunofluorescence and Western blotting assays, DW and TG performed electrophysiology, XW and LZ performed immunofluorescence, LC, YL, and L-MC analyzed the data. WFB provided critical insights for the discussion and data interpretation. LC and L-MC wrote the manuscript. All authors proved the manuscript.

Funding

This work was supported by grants 32271195 (L-MC) and 31571201 (YL) from NSFC as well as grant JCYJ20220530161011025 (L-MC) from Shenzhen Science and Technology Program.

Conflict of interest

The authors declare that the research was conducted in the absence of any commercial or financial relationships that could be construed as a potential conflict of interest.

Publisher's note

All claims expressed in this article are solely those of the authors and do not necessarily represent those of their affiliated organizations, or those of the publisher, the editors and the reviewers. Any product that may be evaluated in this article, or claim that may be made by its manufacturer, is not guaranteed or endorsed by the publisher.

Supplementary material

The Supplementary Material for this article can be found online at: <https://www.frontiersin.org/articles/10.3389/fphys.2023.1154694/full#supplementary-material>

References

- Alper, S. L., Stuart-Tilley, A. K., Biemesderfer, D., Shmukler, B., and Brown, D. (1997). Immunolocalization of AE2 anion exchanger in rat kidney. *Am. J. Physiol.* 273, F601–F614. doi:10.1152/ajprenal.1997.273.4.F601
- Ando, H., Hirose, M., Gainche, L., Kawaai, K., Bonneau, B., Ijuin, T., et al. (2015). IRBIT interacts with the catalytic core of phosphatidylinositol phosphate kinase type Ia and IIa through conserved catalytic aspartate residues. *PLoS One* 10, 01415699. doi:10.1371/journal.pone.0141569
- Ares, G. R., Caceres, P. S., and Ortiz, P. A. (2011). Molecular regulation of NKCC2 in the thick ascending limb. *Am. J. Physiol.-Renal Physiol.* 301, F1143–F1159. doi:10.1152/ajprenal.00396.2011
- Azlan, N. F. M., Koeners, M. P., and Zhang, J. (2021). Regulatory control of the Na-Cl co-transporter NCC and its therapeutic potential for hypertension. *Acta Pharmacol. Sin.* 42, 1117–1128. doi:10.1016/j.apsb.2020.09.009
- Bankir, L., Figueres, L., Prot-Bertoye, C., Bouby, N., Crambert, G., Pratt, J. H., et al. (2020). Medullary and cortical thick ascending limb: Similarities and differences. *Am. J. Physiol.-Renal Physiol.* 318, F422–F442. doi:10.1152/ajprenal.00261.2019
- Barkley, R. A., Chakravarti, A., Cooper, R. S., Ellison, R. C., Hunt, S. C., Province, M. A., et al. (2004). Positional identification of hypertension susceptibility genes on chromosome 2. *Hypertension* 43, 477–482. doi:10.1161/01.HYP.0000111585.76299.f7
- Bazua-Valenti, S., Castaneda-Bueno, M., and Gamba, G. (2016). Physiological role of SLC12 family members in the kidney. *Am. J. Physiol.-Renal Physiol.* 311, F131–F144. doi:10.1152/ajprenal.00071.2016
- Berg, P., Svendsen, S. L., Hoang, T. T. L., Praetorius, H. A., Sorensen, M. V., and Leipziger, J. (2021a). Impaired renal HCO₃⁻ secretion in CFTR deficient mice causes metabolic alkalosis during chronic base-loading. *Acta Physiol.* 231, e13591. doi:10.1111/apha.13591
- Berg, P., Svendsen, S. L., Sorensen, M. V., Schreiber, R., Kunzelmann, K., and Leipziger, J. (2021b). The molecular mechanism of CFTR- and secretin-dependent renal bicarbonate excretion. *J. Physiol.* 599, 3003–3011. doi:10.1113/jp281285
- Boedtker, E., Praetorius, J., Matchkov, V. V., Stankevicius, E., Mogensen, S., Fuchtbauer, A. C., et al. (2011). Disruption of Na⁺,HCO₃⁻ cotransporter NBCn1 (slc4a7) inhibits NO-mediated vasorelaxation, smooth muscle Ca²⁺ sensitivity, and hypertension development in mice. *Circulation* 124, 1819–1829. doi:10.1161/CIRCULATIONAHA.110.015974
- Boger, C. A., Gorski, M., McMahon, G. M., Xu, H., Chang, Y. C., van der Most, P. J., et al. (2017). *NFAT5* and *SLC4A10* loci associate with plasma osmolality. *J. Am. Soc. Nephrol.* 28, 2311–2321. doi:10.1681/ASN.2016080892
- Bourgeois, S., Masse, S., Paillard, M., and Houllier, P. (2002). Basolateral membrane Cl⁻-Na⁺- and K⁺-coupled base transport mechanisms in rat mTALH. *Am. J. Physiol.-Renal Physiol.* 282, F655–F668. doi:10.1152/ajprenal.00220.2000
- Breljak, D., Ljubojevic, M., Hagos, Y., Micek, V., Eror, D. B., Madunic, I. V., et al. (2016). Distribution of organic anion transporters NaDC3 and OAT1-3 along the human nephron. *Am. J. Physiol.-Renal Physiol.* 311, F227–F238. doi:10.1152/ajprenal.00113.2016
- Burckhardt, B. C., Lorenz, J., Kobbe, C., and Burckhardt, G. (2005). Substrate specificity of the human renal sodium dicarboxylate cotransporter, hNaDC-3, under voltage-clamp conditions. *Am. J. Physiol.-Renal Physiol.* 288, F792–F799. doi:10.1152/ajprenal.00360.2004
- Caceres, P. S., and Ortiz, P. A. (2019). Molecular regulation of NKCC2 in blood pressure control and hypertension. *Curr. Opin. Nephrol. Hypertens.* 28, 474–480. doi:10.1097/Mnh.0000000000000551
- Campean, V., Kricke, J., Ellison, D., Luft, F. C., and Bachmann, S. (2001). Localization of thiazide-sensitive Na⁺-Cl⁻ cotransport and associated gene products in mouse DCT. *Am. J. Physiol.-Renal Physiol.* 281, F1028–F1035. doi:10.1152/ajprenal.0148.2001
- Carey, R. M., Schoeffel, C. D., Gillea, J. J., Jones, J. E., McGrath, H. E., Gordon, L. N., et al. (2012). Salt sensitivity of blood pressure is associated with polymorphisms in the sodium-bicarbonate cotransporter. *Hypertension* 60, 1359–1366. doi:10.1161/Hypertensionaha.112.196071
- Chen, L. H., Chou, C. L., and Knepper, M. A. (2021). A comprehensive map of mRNAs and their isoforms across all 14 renal tubule segments of mouse. *J. Am. Soc. Nephrol.* 32, 897–912. doi:10.1681/Asn.2020101406
- Dimke, H., and Schnermann, J. (2018). Axial and cellular heterogeneity in electrolyte transport pathways along the thick ascending limb. *Acta Physiol.* 223, e13057. doi:10.1111/apha.13057
- Ecelbarger, C. A., Terris, J., Hoyer, J. R., Nielsen, S., Wade, J. B., and Knepper, M. A. (1996). Localization and regulation of the rat renal Na⁺-K⁺-2Cl⁻ cotransporter, BSC-1. *Am. J. Physiol.* 271, F619–F628. doi:10.1152/ajprenal.1996.271.3.F619
- Ehret, G. B., Munroe, P. B., Rice, K. M., Bochud, M., Johnson, A. D., Chasman, D. I., et al. (2011). Genetic variants in novel pathways influence blood pressure and cardiovascular disease risk. *Nature* 478, 103–109. doi:10.1038/nature10405
- Gimenez, I., and Forbush, B. (2003). Short-term stimulation of the renal Na-K-Cl cotransporter (NKCC2) by vasopressin involves phosphorylation and membrane translocation of the protein. *J. Biol. Chem.* 278, 26946–26951. doi:10.1074/jbc.M303435200
- Glover, M., Zuber, A. M., Figg, N., and O'Shaughnessy, K. M. (2010). The activity of the thiazide-sensitive Na⁺-Cl⁻ cotransporter is regulated by protein phosphatase PP4. *Can. J. Physiol. Pharmacol.* 88, 986–995. doi:10.1139/y10-080
- Gonzalez-Vicente, A., Saez, F., Monzon, C. M., Asirwatham, J., and Garvin, J. L. (2019). Thick ascending limb sodium transport in the pathogenesis of hypertension. *Physiol. Rev.* 99, 235–309. doi:10.1152/physrev.00055.2017
- Groger, N., Vitzthum, H., Frohlich, H., Kruger, M., Ehmke, H., Braun, T., et al. (2012). Targeted mutation of *SLC4A5* induces arterial hypertension and renal metabolic acidosis. *Hum. Mol. Genet.* 21, 1025–1036. doi:10.1093/hmg/ddr533
- Guo, L., Liu, F., Chen, S., Yang, X., Huang, J., He, J., et al. (2016). Common variants in the Na⁺-coupled bicarbonate transporter genes and salt sensitivity of blood pressure: The GenSalt study. *J. Hum. Hypertens.* 30, 543–548. doi:10.1038/jhh.2015.113
- Guo, Y. M., Liu, Y., Liu, M., Wang, J. L., Xie, Z. D., Chen, K. J., et al. (2017). Na⁺/HCO₃⁻ cotransporter NBCn2 mediates HCO₃⁻ reclamation in the apical membrane of renal proximal tubules. *J. Am. Soc. Nephrol.* 28, 2409–2419. doi:10.1681/ASN.2016080930
- Guyton, A. C. (1989). Dominant role of the kidneys and accessory role of whole-body auto-regulation in the pathogenesis of hypertension. *Am. J. Hyperten.* 2, 575–585. doi:10.1093/Ajh/2.7.575
- He, P. J., Zhao, L. Q., No, Y. R., Karvar, S., and Yun, C. C. (2016). The NHERF1 PDZ1 domain and IRBIT interact and mediate the activation of Na⁺/H⁺ exchanger 3 by ANG II. *Am. J. Physiol.-Renal Physiol.* 311, F343–F351. doi:10.1152/ajprenal.00247.2016
- He, P., Klein, J., and Yun, C. C. (2010). Activation of Na⁺/H⁺ exchanger NHE3 by angiotensin II is mediated by inositol 1,4,5-triphosphate (IP3) receptor-binding protein released with IP3 (IRBIT) and Ca²⁺/calmodulin-dependent protein kinase II. *J. Biol. Chem.* 285, 27869–27878. doi:10.1074/jbc.M110.133066
- He, P., Zhang, H., and Yun, C. C. (2008). IRBIT, inositol 1,4,5-triphosphate (IP3) receptor-binding protein released with IP3, binds Na⁺/H⁺ exchanger NHE3 and activates NHE3 activity in response to calcium. *J. Biol. Chem.* 283, 33544–33553. doi:10.1074/jbc.M805534200
- Hong, J. H., Yang, D., Shcheynikov, N., Ohana, E., Shin, D. M., and Muallem, S. (2013). Convergence of IRBIT, phosphatidylinositol (4,5) bisphosphate, and WNK/SPAK kinases in regulation of the Na⁺-HCO₃⁻ cotransporters family. *Proc. Natl. Acad. Sci. USA.* 110, 4105–4110. doi:10.1073/pnas.1221410110
- Itoh, R., Hatano, N., Murakami, M., Mitsumori, K., Kawasaki, S., Wakagi, T., et al. (2021). Both IRBIT and long-IRBIT bind to and coordinately regulate Cl⁻/HCO₃⁻ exchanger AE2 activity through modulating the lysosomal degradation of AE2. *Sci. Rep.* 11, 5990. doi:10.1038/s41598-021-85499-6
- Ji, W., Foo, J. N., O'Roak, B. J., Zhao, H., Larson, M. G., Simon, D. B., et al. (2008). Rare independent mutations in renal salt handling genes contribute to blood pressure variation. *Nat. Genet.* 40, 592–599. doi:10.1038/ng.118
- Jiang, S., Wang, X. M., Jin, W., Zhang, G. S., Zhang, J., Xie, P., et al. (2019). NaHCO₃ dilates mouse afferent arteriole via Na⁺/HCO₃⁻ cotransporters NBCs. *Hypertension* 74, 1104–1112. doi:10.1161/Hypertensionaha.119.13235
- Kawaai, K., Ando, H., Satoh, N., Yamada, H., Ogawa, N., Hirose, M., et al. (2017). Splicing variation of Long-IRBIT determines the target selectivity of IRBIT family proteins. *Proc. Natl. Acad. Sci. USA.* 114, 3921–3926. doi:10.1073/pnas.1618514114
- Kawaai, K., Mizutani, A., Shoji, H., Ogawa, N., Ebisui, E., Kuroda, Y., et al. (2015). IRBIT regulates CaMKIIα activity and contributes to catecholamine homeostasis through tyrosine hydroxylase phosphorylation. *Proc. Natl. Acad. Sci. USA.* 112, 5515–5520. doi:10.1073/pnas.1503310112
- Khamaysi, A., Anbtawee-Jomaa, S., Fremder, M., Eini-Rider, H., Shimshilashvili, L., Aharon, S., et al. (2019). Systemic succinate homeostasis and local succinate signaling affect blood pressure and modify risks for calcium oxalate lithogenesis. *J. Am. Soc. Nephrol.* 30, 381–392. doi:10.1681/ASN.2018030277
- Kikeri, D., Azar, S., Sun, A., Zeidel, M. L., and Hebert, S. C. (1990). Na⁺-H⁺ antiporter and Na⁺-(HCO₃⁻)_n symporter regulate intracellular pH in mouse medullary thick limbs of Henle. *Am. J. Physiol.* 258, F445–F456. doi:10.1152/ajprenal.1990.258.3.F445
- Kim, Y. H., Kwon, T. H., Christensen, B. M., Nielsen, J., Wall, S. M., Madsen, K. M., et al. (2003). Altered expression of renal acid-base transporters in rats with lithium-induced NDI. *Am. J. Physiol.-Renal Physiol.* 285, F1244–F1257. doi:10.1152/ajprenal.00176.2003
- Knauf, F., Velazquez, H., Pfann, V., Jiang, Z., and Aronson, P. S. (2019). Characterization of renal NaCl and oxalate transport in Slc26a6^{-/-} mice. *Am. J. Physiol.-Renal Physiol.* 316, F128–F133. doi:10.1152/ajprenal.00309.2018
- Knauf, F., Yang, C. L., Thomson, R. B., Mentone, S. A., Giebisch, G., and Aronson, P. S. (2001). Identification of a chloride-formate exchanger expressed on the brush border membrane of renal proximal tubule cells. *Proc. Natl. Acad. Sci. USA.* 98, 9425–9430. doi:10.1073/pnas.141241098
- Kokubo, Y., Tomoike, H., Tanaka, C., Banno, M., Okuda, T., Inamoto, N., et al. (2006). Association of sixty-one non-synonymous polymorphisms in forty-one hypertension candidate genes with blood pressure variation and hypertension. *Hypertens. Res.* 29, 611–619. doi:10.1291/hypres.29.611

- Lee, H.-W., Handlogten, M. E., Osis, G., Clapp, W. L., Wakefield, D. N., Verlander, J. W., et al. (2017). Expression of sodium-dependent dicarboxylate transporter 1 (NaDC1/SLC13A2) in normal and neoplastic human kidney. *Am. J. Physiol.-Renal Physiol.* 312, F427–F435. doi:10.1152/ajprenal.00559.2016
- Lee, S. K., and Boron, W. F. (2018). Exploring the autoinhibitory domain of the electrogenic Na⁺/HCO₃⁻ transporter NBCe1-B, from residues 28 to 62. *J. Physiol.* 596, 3637–3653. doi:10.1113/JP276241
- Lee, S. K., Boron, W. F., and Parker, M. D. (2012). Relief of autoinhibition of the electrogenic Na-HCO₃ cotransporter NBCe1-B: Role of IRBIT vs. amino-terminal truncation. *Am. J. Physiol.-Cell Physiol.* 302, C518–C526. doi:10.1152/ajpcell.00352.2011
- Liu, Y., Wang, D. K., Jiang, D. Z., Qin, X., Xie, Z. D., Wang, Q. K., et al. (2013). Cloning and functional characterization of novel variants and tissue-specific expression of alternative amino and carboxyl termini of products of Slc4a10. *PLoS One* 8, e55974. doi:10.1371/journal.pone.0055974
- Liu, Y., Yang, J., and Chen, L. M. (2015). Structure and function of SLC4 family HCO₃⁻ transporters. *Front. Physiol.* 6, 355. doi:10.3389/fphys.2015.00355
- Lu, X., Wang, L., Lin, X., Huang, J., Charles Gu, C., He, M., et al. (2015). Genome-wide association study in Chinese identifies novel loci for blood pressure and hypertension. *Hum. Mol. Genet.* 24, 865–874. doi:10.1093/hmg/ddu478
- McAlear, S. D., Liu, X., Williams, J. B., McNicholas-Bevensee, C. M., and Bevensee, M. O. (2006). Electrogenic Na/HCO₃ cotransporter (NBCe1) variants expressed in *Xenopus* oocytes: Functional comparison and roles of the amino and carboxy termini. *J. Gen. Physiol.* 127, 639–658. doi:10.1085/jgp.200609520
- Murthy, M., Kurz, T., and O'Shaughnessy, K. M. (2017). WNK signalling pathways in blood pressure regulation. *Cell. Mol. Life Sci.* 74, 1261–1280. doi:10.1007/s00018-016-2402-z
- Mutig, K. (2017). Trafficking and regulation of the NKCC2 cotransporter in the thick ascending limb. *Curr. Opin. Nephrol. Hypertens.* 26, 392–397. doi:10.1097/Mnh.0000000000000351
- Nwia, S. M., Li, X. C., Leite, A. P. d. O., Hassan, R., and Zhuo, J. L. (2022). The Na⁺/H⁺ exchanger 3 in the intestines and the proximal tubule of the kidney: Localization, physiological function, and key roles in angiotensin II-induced hypertension. *Front. Physiol.* 13, 861659. doi:10.3389/fphys.2022.861659
- Odgaard, E., Jakobsen, J. K., Frische, S., Praetorius, J., Nielsen, S., Aalkjaer, C., et al. (2004). Basolateral Na⁺-dependent HCO₃⁻ transporter NBCn1-mediated HCO₃⁻ influx in rat medullary thick ascending limb. *J. Physiol.* 555, 205–218. doi:10.1113/jphysiol.2003.046474
- Ohana, E., Shcheynikov, N., Moe, O. W., and Muallem, S. (2013). SLC26A6 and NaDC-1 transporters interact to regulate oxalate and citrate homeostasis. *J. Am. Soc. Nephrol.* 24, 1617–1626. doi:10.1681/Asn.2013010080
- Park, S., Shcheynikov, N., Hong, J. H., Zheng, C., Suh, S. H., Kawaai, K., et al. (2013). IRBIT mediates synergy between Ca²⁺ and cAMP signaling pathways during epithelial transport in mice. *Gastroenterology* 145, 232–241. doi:10.1053/j.gastro.2013.03.047
- Parker, M. D., and Boron, W. F. (2013). The divergence, actions, roles, and relatives of sodium coupled bicarbonate transporters. *Physiol. Rev.* 93, 803–959. doi:10.1152/physrev.00023.2012
- Penton, D., Moser, S., Wengi, A., Czogalla, J., Rosenbaek, L. L., Rigendinger, F., et al. (2019). Protein phosphatase 1 inhibitor-1 mediates the cAMP-dependent stimulation of the renal NaCl cotransporter. *J. Am. Soc. Nephrol.* 30, 737–750. doi:10.1681/asn.2018050540
- Peti-Peterdi, J., and Harris, R. C. (2010). Macula densa sensing and signaling mechanisms of renin release. *J. Am. Soc. Nephrol.* 21, 1093–1096. doi:10.1681/Asn.2009070759
- Picard, N., Trompf, K., Yang, C. L., Miller, R. L., Carrel, M., Loffing-Cueni, D., et al. (2014). Protein phosphatase 1 inhibitor-1 deficiency reduces phosphorylation of renal NaCl cotransporter and causes arterial hypotension. *J. Am. Soc. Nephrol.* 25, 511–522. doi:10.1681/Asn.2012121202
- Poulsen, S. B., Cheng, L., Penton, D., Kortenoeven, M. L. A., Matchkov, V. V., Loffing, J., et al. (2021). Activation of the kidney sodium chloride cotransporter by the beta 2-adrenergic receptor agonist salbutamol increases blood pressure. *Kidney Intl* 100, 321–335. doi:10.1016/j.kint.2021.04.021
- Praetorius, J., Kim, Y. H., Bouzinova, E. V., Frische, S., Rojek, A., Aalkjaer, A., et al. (2004). NBCn1 is a basolateral Na⁺-HCO₃⁻ cotransporter in rat kidney inner medullary collecting ducts. *Am. J. Physiol.-Renal Physiol.* 286, F903–F912. doi:10.1152/ajprenal.00437.2002
- Quentin, F., Eladari, D., Frische, S., Cambillau, M., Nielsen, S., Alper, S.L., et al. (2004). Regulation of the Cl⁻/HCO₃⁻ exchanger AE2 in rat thick ascending limb of Henle's loop in response to changes in acid-base and sodium balance. *J. Am. Soc. Nephrol.* 15, 2988–2997. doi:10.1097/01.ASN.0000146426.93319.16
- Richardson, C., and Alessi, D. R. (2008). The regulation of salt transport and blood pressure by the WNK-SPAK/OSR1 signalling pathway. *J. Cell Sci.* 121, 3293–3304. doi:10.1242/jcs.029223
- Shao, S., Li, X.-D., Lu, Y.-Y., Li, S.-J., Chen, X.-H., Zhou, H.-D., et al. (2021). Renal natriuretic peptide receptor-C deficiency attenuates NaCl cotransporter activity in angiotensin II-induced hypertension. *Hypertension* 77, 868–881. doi:10.1161/hypertensionaha.120.15636
- Shekarabi, M., Zhang, J., Khanna, A. R., Ellison, D. H., Delpire, E., and Kahle, K. T. (2017). WNK kinase signaling in ion homeostasis and human disease. *Cell Metab.* 25, 285–299. doi:10.1016/j.cmet.2017.01.007
- Shirakabe, K., Priori, G., Yamada, H., Ando, H., Horita, S., Fujita, T., et al. (2006). IRBIT, an inositol 1,4,5-trisphosphate receptor-binding protein, specifically binds to and activates pancreas-type Na⁺/HCO₃⁻ cotransporter 1 (pNBC1). *Proc. Natl. Acad. Sci. USA.* 103, 9542–9547. doi:10.1073/pnas.0602250103
- Sober, S., Org, E., Kepp, K., Juhanson, P., Eyheramendy, S., Gieger, C., et al. (2009). Targeting 160 candidate genes for blood pressure regulation with a genome-wide genotyping array. *PLoS One* 4, e6034. doi:10.1371/journal.pone.0006034
- Su, P., Wu, H., Wang, M., Cai, L., Liu, Y., and Chen, L. M. (2021). IRBIT activates NBCe1-B by releasing the auto-inhibition module from the transmembrane domain. *J. Physiol.* 599, 1151–1172. doi:10.1113/JP280578
- Torres-Pinzon, D. L., Ralph, D. L., Veiras, L. C., and McDonough, A. A. (2021). Sex-specific adaptations to high-salt diet preserve electrolyte homeostasis with distinct sodium transporter profiles. *Am. J. Physiol.-Cell Physiol.* 321, C897–C909. doi:10.1152/ajpcell.00282.2021
- Tran, T. M., Park, M. Y., Lee, J., Bae, J. S., Hwang, S. M., Choi, S. Y., et al. (2013). IRBIT plays an important role in NHE3-mediated pH_i regulation in HSG cells. *Biochem. Biophys. Res. Commun.* 437, 18–22. doi:10.1016/j.bbrc.2013.06.010
- Trudeau, M. C., Warmke, J. W., Ganetzky, B., and Robertson, G. A. (1995). HERG, a human inward rectifier in the voltage-gated potassium channel family. *Science* 269, 92–95. doi:10.1126/science.7604285
- Wadei, H. M., and Textor, S. C. (2012). The role of the kidney in regulating arterial blood pressure. *Nat. Rev. Nephrol.* 8, 602–609. doi:10.1038/nrneph.2012.191
- Wang, J. L., Wang, X. Y., Wang, D. K., Parker, M. D., Musa-Aziz, R., Popple, J., et al. (2020a). Multiple acid-base and electrolyte disturbances upregulate NBCn1, NBCn2, IRBIT and L-IRBIT in the mTAL. *J. Physiol.* 598, 3395–3415. doi:10.1113/JP279009
- Wang, L., Li, H., Yang, B., Guo, L., Han, X., Li, L., et al. (2017). The hypertension risk variant rs820430 functions as an enhancer of SLC4A7. *Am. J. Hypertens.* 30, 202–208. doi:10.1093/ajh/hpw127
- Wang, M., Wu, H., Liu, Y., and Chen, L.-M. (2020b). Activation of mouse NBCe1-B by *Xenopus laevis* and mouse IRBITs: Role of the variable Nt appendage of IRBITs. *BBA-Biomembranes.* 1862, 183240. doi:10.1016/j.bbamem.2020.183240
- Wetzel, R. K., and Sweadner, K. J. (2001). Immunocytochemical localization of Na-K-ATPase alpha- and gamma-subunits in rat kidney. *Am. J. Physiol.-Renal Physiol.* 281, F531–F545. doi:10.1152/ajprenal.2001.281.3.F531
- Yamaguchi, S., and Ishikawa, T. (2014). AHCYL2 (long-IRBIT) as a potential regulator of the electrogenic Na⁺-HCO₃⁻ cotransporter NBCe1-B. *FEBS Lett.* 588, 672–677. doi:10.1016/j.febslet.2013.12.036
- Yang, H. C., Liang, Y. J., Chen, J. W., Chiang, K. M., Chung, C. M., Ho, H. Y., et al. (2012). Identification of IGF1, SLC4A4, WWOX, and SFMBT1 as hypertension susceptibility genes in Han Chinese with a genome-wide gene-based association study. *PLoS One* 7, e32907. doi:10.1371/journal.pone.0032907